

RXTE Observation of Cygnus X-1: Spectra and Timing

J. Wilms¹, J. Dove², M. Nowak², B. A. Vaughan³

¹IAA Tübingen, Astronomie, Waldhäuser Str. 64, D-72076 Tübingen

²JILA, University of Colorado, Campus Box 440, Boulder, CO 80309-0440

³Space Radiation Laboratory, Caltech, Pasadena, CA 91125

Abstract

We present first results from the analysis of an RXTE observation of Cyg X-1 in its low state, taken about two months after the end of the high state. With $\Gamma \approx 1.45$ the spectrum is considerably harder than previous low-state measurements. The observed spectrum can be explained by a Comptonization spectrum as that emitted from a spherical corona surrounded by a cold accretion disk. The optical depth of the corona is between 2 and 2.5 and the temperature is between 60 and 80 keV. Temporal analysis shows a typical RMS noise of $\approx 25\%$. The PSD can be described as consisting of a flat component followed by an f^{-1} power-law, followed by an $f^{-1.6}$ power law. The lag of the hard photons with respect to the soft photons is consistent with prior observations. The coherence function is remarkably close to unity from 0.01 Hz to 10 Hz.

Data Analysis

The observation presented here was made on October 23/24, 1996. The total time on-source was 19 ksec, due to missing data only 10 ksec were used for the spectral analysis. The source count-rates were ≈ 4300 counts/sec for PCA and ≈ 170 counts/sec in each HEXTE cluster. The data were analyzed using FTOOLS 3.6.1, using the newest HEXTE response-matrix and the pre-FTOOLS 3.6.1 response matrices for PCA^a. We added a systematic error of 1% to the PCA data to account for the existing uncertainties in the PCA-RMF and fitted the PCA spectrum between 4 keV and 30 keV. The background for PCA was determined from Earth occultation observations as well as from backgrounds estimated using pcabackest. The results presented here are insensitive to which method is used to generate the background.

^aThe newest pcarmf has only been released for SunOS; we are still waiting for a release that is suitable for OSF/1 machines.

The Sphere+Disk Model

We have developed an accretion disk corona (ADC) model to self-consistently calculate the spectrum, the temperature structure, and the pair-opacity of the corona for several morphologies (Dove et al. 1997a,b). The computed spectra have been implemented into XSPEC and are publically available upon request.

Models in which the corona lies directly above the accretion disk (“slab geometry”) are unable to explain the observed X-ray spectrum of Cyg X-1 since the coronal temperatures are too low causing the spectrum to be too soft to explain the data. On the other hand, a model in which a hot spherical corona sits in the center of an external cold accretion disk, appears to be able to describe the observed spectrum (“sphere+disk model”; Dove et al. 1997b).

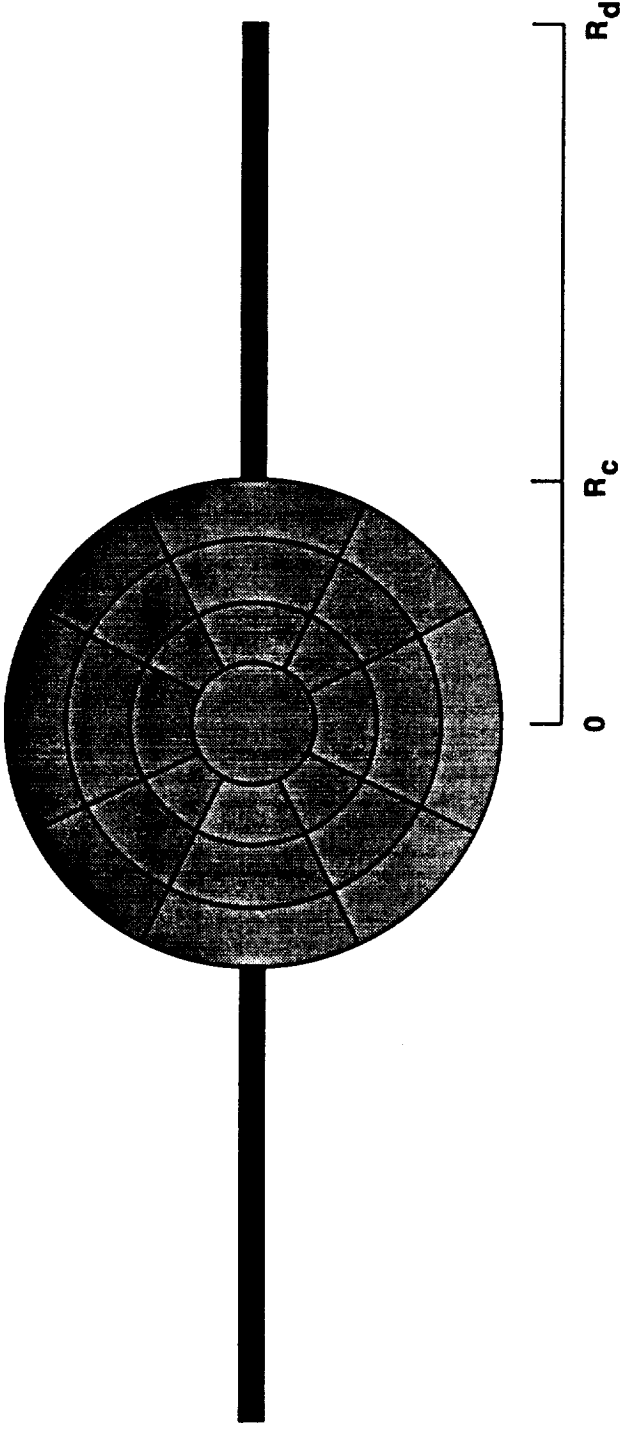


Figure 1: The sphere+disk geometry. The corona has an optical depth $\tau = n_e \sigma_T R_c$ and is subdivided into zones in which the local coronal properties are determined self-consistently. The seed-photons for Comptonization are emitted by the cold accretion disk which also serves as the reprocessing medium.

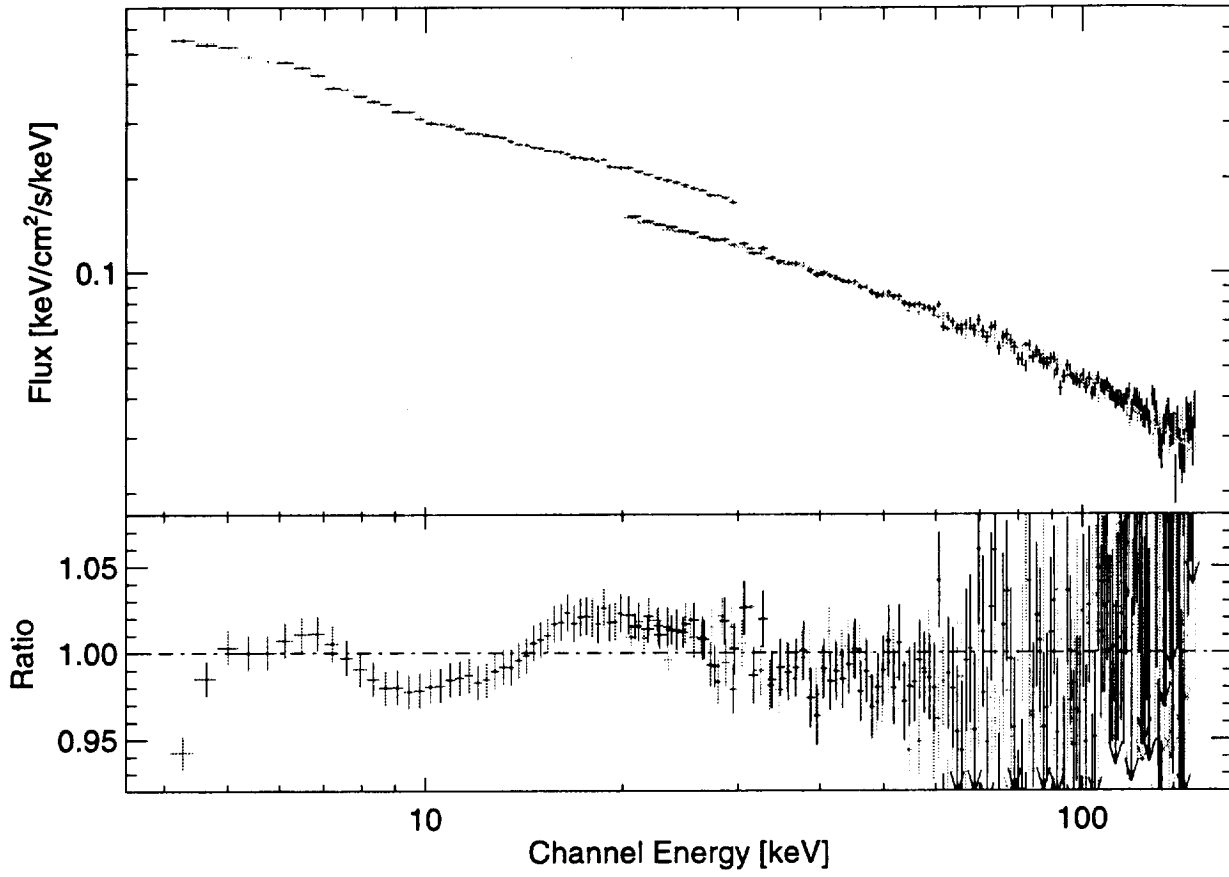


Figure 2: Comparison of the RXTE spectrum to the best-fit sphere+disk model. Here, the optical depth of the sphere is 2.6 and the temperature is 60 keV. The temperature of the accretion disk was assumed to be $T(r) = 300 \text{ keV} \cdot r^{-0.75}$ where $r = (R/R_c)$ (see fig. 1) and N_H was fixed at $6 \times 10^{21} \text{ cm}^{-2}$.

Spectral Results

N_{H} 10^{21} cm^{-2}	Power Law / Cutoff		Black Body		Refl.	ADC	
	Γ	E_{fold} keV	kT_{BB} eV	A^a	f_{cov}^b	τ	χ^2/dof
6.0 ^d	1.53	200					1451.0/300
0.0	1.53	200					1224.0/299
6.0	1.49	200	929	0.07			443.1/298
42.0	1.5	200	855	0.11			367.9/297
6.0	1.46	179	1060	0.10	0.10		267.2/297
6.0	1.52	215	800	0.15	0.10		401.8/298
6.0			853	0.05		0.7 89	659.2/298 ^e
6.0						1.8 82	458.0/300 ^f
32.0			739	0.06		1.8 82	267.9/297 ^f
6.0			830	0.03		2.0 82	306.8/298 ^f
6.0						2.6 60	487.9/300 ^g
6.0			900	0.0		2.6 60	487.9/300 ^g
17.0						2.5 60	421.1/299 ^g
53.0			677	0.05		2.5 60	331.0/297 ^g
6.0						2.1 65	369.3/300 ^h
6.0						0.3 110	310000./300 ⁱ

^a Ratio between the black-body flux and the total flux from 4 to 30 keV.

^b Relative normalization of the reflection component to the direct component.

^c Coronal temperature.

^d Values set in *italics* have been fixed.

^e Comptonization model, slab geometry, from Hua & Titarchuk (1995).

^f ADC model with sphere+disk geometry; $kT_{\text{disk}} = 50 \text{ keV}$.

^g ADC model with sphere+disk geometry; $kT_{\text{disk}} = 300 \text{ keV} \cdot (R/R_c)^{-0.75}$.

^h ADC model with sphere+disk geometry; $kT_{\text{disk}} = 150 \text{ keV} \cdot (R/R_c)^{-0.75}$.

ⁱ ADC model with slab geometry; $kT_{\text{disk}} = 200 \text{ eV}$.

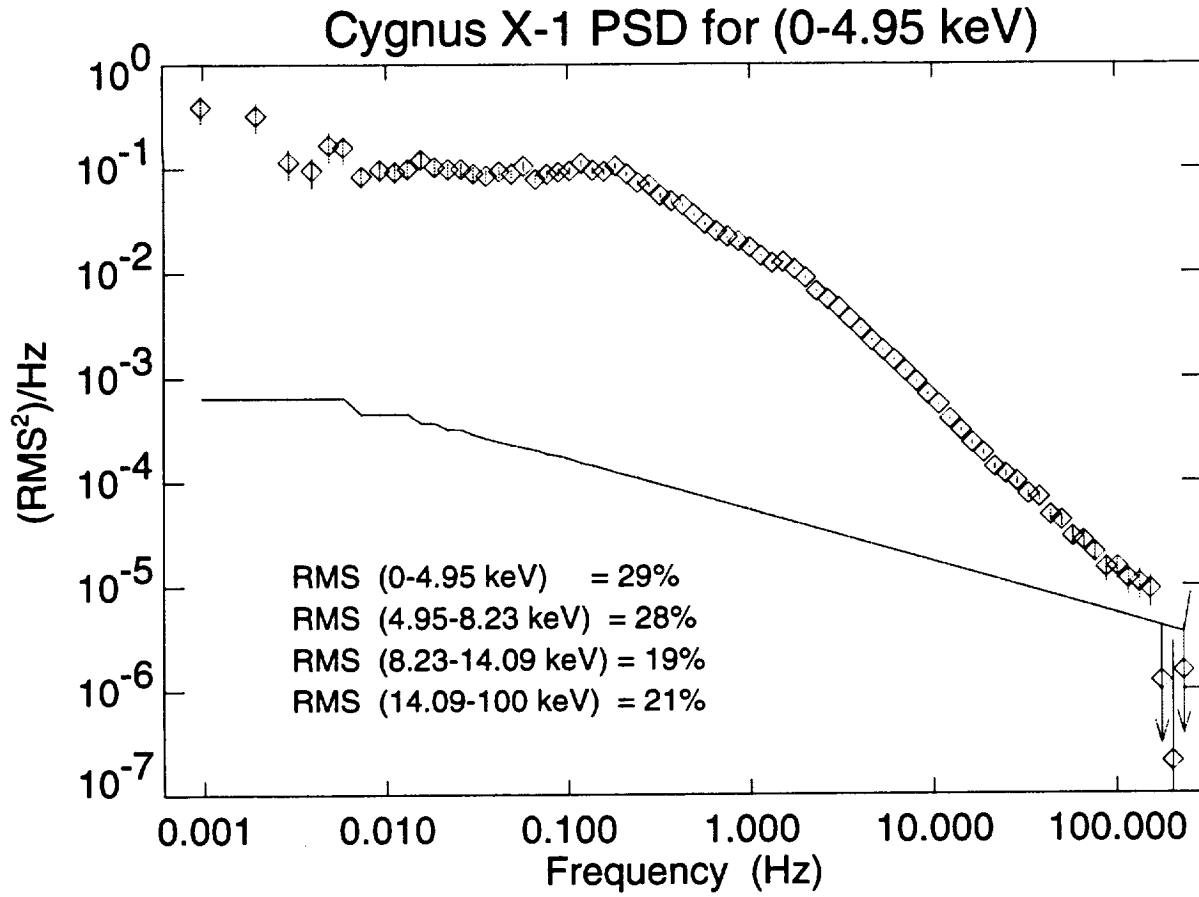


Figure 3: PSD for the energy-band below 5 keV for a 10 ks observation. The rms-noise has been subtracted from the PSD, the sensitivity-level of which is indicated by the thin line. Normalization follows Miyamoto et al. (1992).

The PSD can be roughly described as

$$\frac{\text{PSD}}{\text{rms}^2/\text{Hz}} = \begin{cases} 0.091 & \text{for } f < 0.2 \text{ Hz} \\ 0.017 f^{-1.04} & \text{for } 0.2 \text{ Hz} \leq f < 2.4 \text{ Hz} \\ 0.031 f^{-1.71} & \text{for } 2.4 \text{ Hz} \leq f \end{cases}$$

where the break frequencies and power-law slopes have been determined numerically.

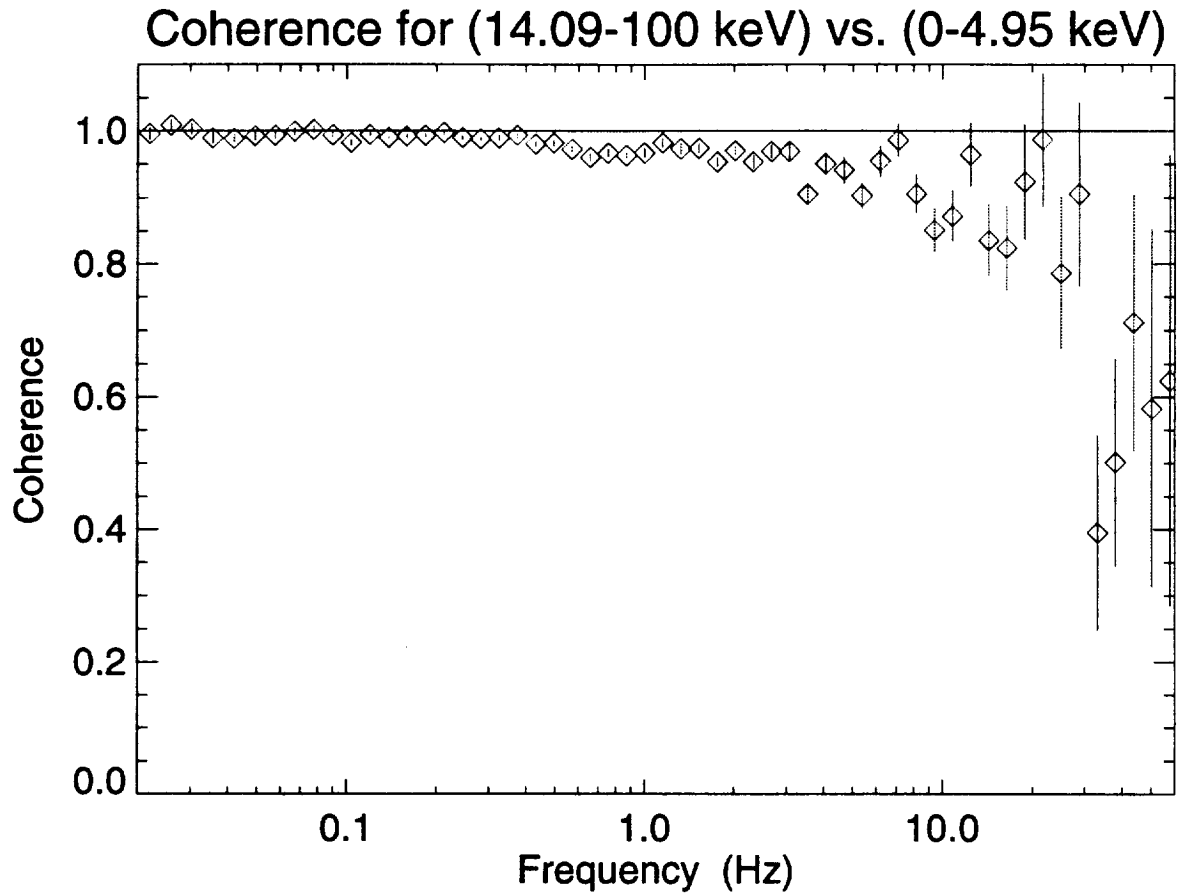


Figure 4: *Coherence between the hard and soft energies.*

The coherence function (Nowak & Vaughan (1996); Vaughan & Nowak (1997)) is defined as

$$\gamma^2(f) = \frac{|\langle C(f) \rangle|^2}{\langle |S_1(f)|^2 \rangle \langle |S_2(f)|^2 \rangle}$$

where $C(f)$ is the cross-spectrum between the two observed signals $X_i(f) = S_i(f) + N_i(f)$, where $S_i(f)$ is the true signal and $N_i(f)$ is the Poisson noise-component (“observational rms noise”). The measured coherence of unity from 0.01 Hz to 10 Hz indicates a remarkable stability in the timing properties of the signal over the whole spectrum — an indication that either there is a single global source for the observed fluctuations, or that there is a global coherent response from the Compton corona, or both (Nowak et al. 1996).

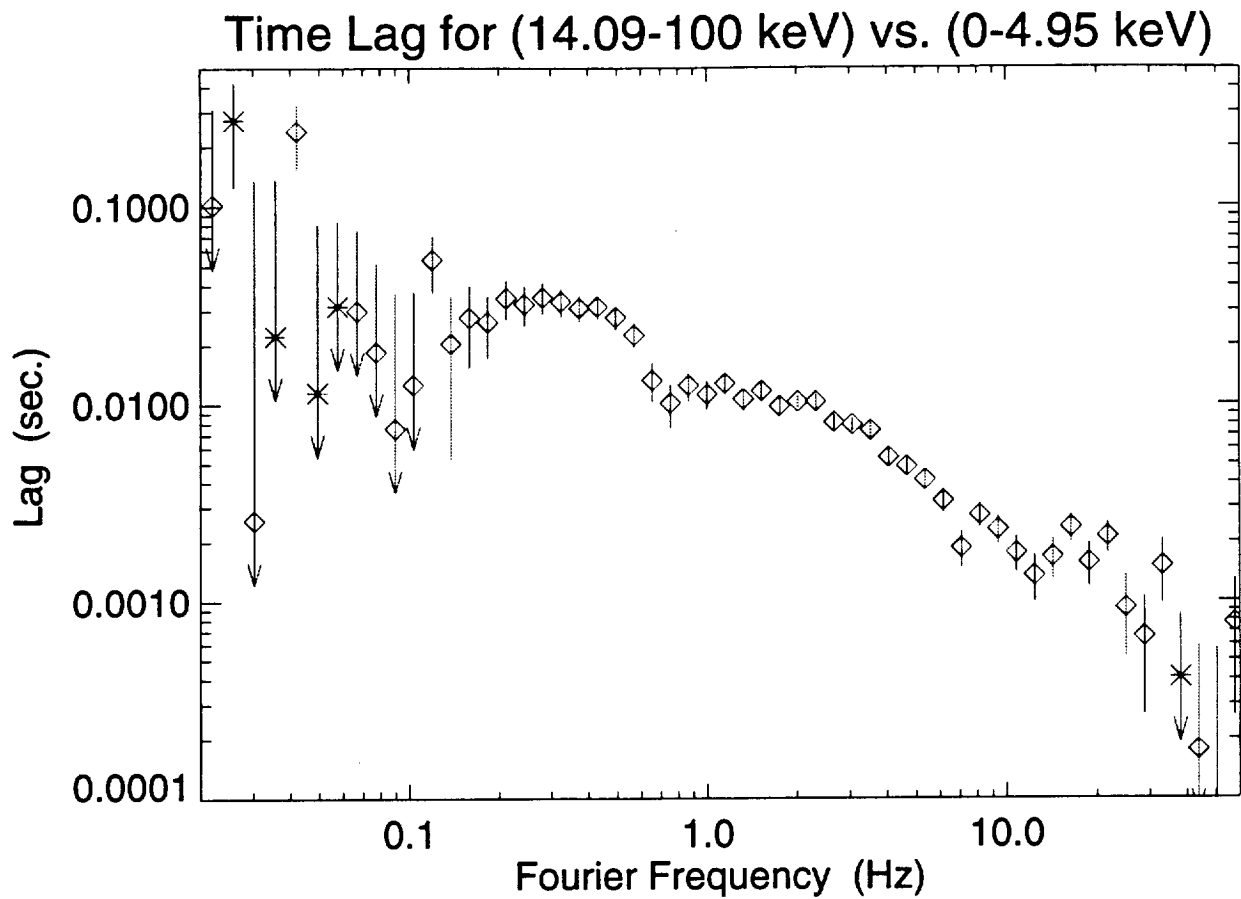


Figure 5: Time lag measured between the hard and the soft energy band. Red: the hard band lags the soft band, Blue: soft band lags the hard band.

The time-lag is well determined in the regime where the coherence function is unity, i.e., 0.01 Hz to 10 Hz. Above ≈ 10 Hz the coherence is not preserved and therefore the time-lag varies erratically. The kinks at 0.8 Hz and ≈ 15 Hz are real (Miyamoto et al. 1992).

Where are the Compton Lags?

If you've read the abstracts volume you might be looking for a poster on theoretical computations of Compton Time Lags and the Coherence function. We deemed the observations presented here to be more important for the poster — but if you have a different opinion, please enter your name in the list below and we will send you information about the originally planned poster (or just sign in if you want preprints):

Name	Address / email	Name	Address / email

References

- Dove, J. B., Wilms, J., Begelman, M. C., 1997a, ApJ, accepted
- Dove, J. B., Wilms, J., Maisack, M. G., Begelman, M. C., 1997b, ApJ, accepted
- Hua, X.-M., Titarchuk, L., 1995, ApJ, 449, 188
- Miyamoto, S., Kitamoto, S., Iga, S., et al., 1992, ApJ, 391, L21
- Nowak, M. A., Vaughan, B. A., 1996, MNRAS, 280, 227
- Nowak, M. A., Vaughan, B. A., Dove, J., Wilms, J., 1996, in D. Wickramasinghe, L. Ferrario, G. Bicknell (eds.), Accretion Phenomena and Related Outflows, IAU Coll. 163, in press
- Vaughan, B. A., Nowak, M. A., 1997, ApJ, 474, L43

